Thermochimica Acta 499 (2010) 21–26

Contents lists available at ScienceDirect

Thermochimica Acta

journal homepage: www.elsevier.com/locate/tca

# Thermal decomposition of supported lithium nitrate catalysts

Maria Lucia Ruiz[a], Ileana Daniela Lick[b,*], Marta Isabel Ponzi[a], Enrique Rodríguez Castellón[c], Antonio Jiménez-López[c], Esther Natalia Ponzi[b]

[a] INTEQUI (CONICET-UNSL), 25 de Mayo 384, V. Mercedes, 5730, San Luis, Argentina
[b] CINDECA (CONICET-UNLP), Calle 47 N◦ 257, La Plata, 1900, Buenos Aires, Argentina
[c] Departamento de Química Inorgánica, Cristalografía y Mineralogía. Facultad de Ciencias, Universidad de Málaga, Campus de Teatinos, 29071 Málaga, Spain

ARTICLE INFO

*Article history:*
Received 10 June 2009
Received in revised form 27 October 2009
Accepted 29 October 2009
Available online 4 November 2009

*Keywords:*
Soot combustion
Silica
Zirconia
Lithium nitrate

ABSTRACT

New catalysts for soot combustion were prepared by impregnation of different supports ($SiO_2$, $ZrO_2$ and $ZrO_2 \cdot nH_2O$) with a $LiNO_3$ solution and then characterized by means of FTIR, XPS, TGA and UV–vis spectroscopy, whereby the presence of lithium nitrate in the prepared catalysts was identified and quantified. The soot combustion rate using this series of catalysts ($LiNO_3$/support) was compared with the activity of a series of impregnated catalysts prepared using LiOH ($Li_2O$/supports). Catalysts prepared using $LiNO_3$ are found to be more active than those prepared using LiOH. The catalytic performance was also studied with a $NO/O_2$ mixture in the feed, demonstrating that NO increases the combustion rate of soot, probably as a consequence of lithium oxide forming an “in situ” nitrate ion.

## 1. Introduction

Diesel engines are widely used for several applications, but mainly for transport in light and heavy vehicles, since they combine inexpensive fuel, with high durability, lower $CO_2$ emissions than gasoline engines and a low maintenance cost. However, the disadvantage of this type of engine is that they generate insalubrious pollution [1]. The principal contaminants emitted by this type of engine are nitrogen oxides and soot [2].

When a catalytic reaction is of the solid–solid–gas type, as occurs in the combustion of soot with $O_2$ in the presence of a solid catalyst, the contact between the catalyst and the soot is a key factor for the reaction that occurs in a soot–catalyst–$O_2$ interface. Such an interface is created by the molten salt types $Cs_2SO_4–V_2O_5$, $CsVO_3–MoO_3$, $Cs_2O–V_2O_5$ [3–5] and $LiNO_3$, $KNO_3$, $CsNO_3$ [6].

$KNO_3$ catalysts supported on zirconia [7] have the same catalytic behavior when samples of soot–catalysts are either milled together in a mortar, termed “tight contact”, or when they are mixed with a spatula, termed “loose contact”. In general, catalysts based on alkaline nitrates that melt at low temperature are excellent catalysts even when they operate with low mechanical contact, or “loose contact”. The results from this study show that this salt provides a good contact between the catalyst and soot, attributed to the wetting of the soot by the catalyst. Similar observations were recently reported in a detailed study performed by Setiabudi et al. using the microscopy technique [8], in which it is possible to observe how the catalyst wets the soot while also providing a combustion interface.

An additional property displayed by catalysts containing nitrates of alkaline metals is the redox property. The nitrate anion can be reduced in the catalytic process to nitrite [9,10].

$$2\,KNO_3 + C(soot) \rightarrow 2\,KNO_2 + CO_2 \qquad (1)$$

$$2\,KNO_2 + O_2 \rightarrow 2\,KNO_3 \qquad (2)$$

Catalysts made using alkaline nitrates have the unfavorable property of losing their active phase during the combustion process. Aging studies with catalysts containing a series of nitrates of alkaline metals ($LiNO_3$, $KNO_3$ and $CsNO_3$) show that catalysts containing lithium nitrate are the most stable with respect to aging in water vapor flow [11].

In this work, the influence of different species on the catalytic combustion of soot with catalysts containing lithium nitrate impregnated on zirconium hydroxides, zirconium oxide and silica are studied. $ZrO_2$ and $ZrO_2 \cdot nH_2O$ have been selected by the high mobility of the oxygen in this oxide and because it is a moderately active material for the carbon combustion reaction [12,13]. Silica has been selected due to the large surface area it offers as an inert support.

---

* Corresponding author.
*E-mail address:* eponzi@quimica.unlp.edu.ar (E.N. Ponzi).

0040-6031/$ – see front matter © 2009 Elsevier B.V. All rights reserved.
doi:10.1016/j.tca.2009.10.016

## 2. Experimental

### 2.1. Preparation of the $ZrO_2·nH_2O$ support

The hydrated zirconium oxide used as a support was obtained from the hydrolysis of zirconium oxychloride, $ZrOCl_2·6H_2O$ (Fluka). Aqueous ammonium hydroxide was added to the zirconium salt solution until pH 10 was reached. Mechanical stirring was used to achieve a good homogeneity. The resulting gel was left to rest for 24 h. The formed precipitate was filtered and washed up to non-identification of the ion chloride in the washing water, and finally the material was dried at 110 °C for 24 h. The solid obtained was milled in a mortar and sieved to obtain particle sizes between 0.150 and 0.090 mm.

### 2.2. Preparation of precursors and catalysts

For the preparation of the lithium nitrate precursors, the support impregnation was carried out with an aqueous solution of 4.2% (w/v) lithium nitrate in a rotovapor equipment operating with a $T_{bath}$ = 100 °C, at a rate of 170 rpm and a vacuum pressure of 500 mmHg. Precursors are denoted with the prefix P ($PLiNO_3/SiO_2$, $PLiNO_3/ZrO_2$ and $PLiNO_3/ZrO_2·nH_2O$, respectively). Precursors once impregnated were dried at 80 °C for 2 h and subsequently calcined at 600 °C for 1 h. The calcination temperature of precursors was selected approximately 200 °C above the operation temperature of catalysts in an exhaust pipe. This calcination temperature also ensures that catalyst transformations do not occur during the catalytic test. In order to differentiate zirconia supports, $ZrO_2$ represents the catalyst impregnated on the oxide, and $ZrO_{2(tetra)}$ represents the catalyst prepared by impregnation of the zirconium hydroxide ($LiNO_3/SiO_2$, $LiNO_3/ZrO_2$ and $LiNO_3/ZrO_{2(tetra)}$). The nominal concentration of nitrate ions in all catalysts was 7.5% (w/w), or 8.34% (w/w) when expressed as lithium nitrate.

For the preparation of catalysts with LiOH, the same technique was used with the nomenclature being $Li_2O/SiO_2$, $Li_2O/ZrO_2$ and $Li_2O/ZrO_{2(tetra)}$.

### 2.3. Characterization of catalysts

The concentration of nitrates was determined using a colorimetric technique. A sample of 100 mg of catalyst was washed several times with tri-distilled water, and the resulting solution was measured in a colorimeter DR/890 Hach. The results are expressed as % (w/w) of nitrate ions. The lithium content was determined by atomic absorption spectrometry with an AAnalyst 800 (Perkin-Elmer).

Samples were also studied by XPS with a Physical Electronics PHI-750 spectrometer, equipped with a Mg-$K_\alpha$ (1253.6 eV) X-ray source. In order to measure the binding energies ($\alpha$ 0.1 eV), the signal of adventitious C 1s that appears at 284.8 eV was used as a reference. All samples were outgassed previous to analysis for 12 h under ultra-high vacuum ($<1.3 \times 10^{-6}$ Pa).

The identification of the crystalline species, in precursors and catalysts, was carried out by XRD in a Rigaku equipment, model D-Max III C, operating with Cu K$\alpha$ radiation, Ni filter, 30 kV and 20 mA. The nitrate presence in the catalysts was recorded by means of FTIR with a Spectrum RX1 (Perkin-Elmer) equipment.

### 2.4. Thermal transformations of $LiNO_3$ (bulk and precursors)

Thermal transformations in mass (decomposition, volatilization) that could occur in precursors were analyzed by means of thermogravimetric analysis (Shimadzu TGA-50). For these experiments, 10 mg of solid was used, the gaseous feed (60 $cm^3 min^{-1}$) contained air (40 ml $min^{-1}$) and helium (20 ml $min^{-1}$), the heating rate used was 10 °C $min^{-1}$ and the final temperature was between 600 and 800 °C.

Decomposition gaseous products were analyzed by mass spectroscopy with an on-line Dycor–Ametek mass spectrometer.

Other thermal transformations (melting) that could occur in precursors and catalysts were analyzed by differential scanning calorimetry (Shimadzu DSC-50). The mass used in experiments was 10 mg, the carrier gas was nitrogen and the final temperature was 500 °C. The DSC unit was calibrated using zinc.

### 2.5. Measurements of catalytic activity

Two types of equipment were used to carry out the catalytic experiments; a thermogravimetric reactor with an air/inert feed and a fixed bed reactor with an oxygen/nitric, oxide/inert or oxygen/inert gas feed.

In the first case, activity measurements were carried out in a thermogravimetric equipment, with a total flow of 60 $cm^3 min^{-1}$ and an air:helium ratio of 2:1 with a heating rate 10 °C $min^{-1}$. The catalyst (30 mg) and soot (3 mg) (Printex-U, Degussa) were milled in an agate mortar for 2 min to obtain a good contact, then 11 mg of mixture were placed in the thermobalance cell. The derivative curve (DTG) was obtained from the mass loss information as a function of time, and from this curve, at the minimum in DTG curve, the temperature of maximum rate of soot combustion (Tmax) is determined.

In the second case, the catalytic tests were performed in a flow reactor with an analysis of the reaction gases. The flow reactor was fixed bed, constructed in quartz (id = 0.8 cm) and heated electrically with the temperature measured by means of a K type thermocouple in contact with the catalytic bed. The reaction mixture was obtained from three controlled individually feed lines: NO/He, $O_2$/He and He to adjust the balance (0 or 1500 ppm of NO and 8% of $O_2$). The Total flow used was 50 ml $min^{-1}$. The microreactor was loaded with 33 mg of “loose contact” catalyst-soot mixture (30 mg of catalyst and 3 mg of soot) and oxidation was carried out in the range of 200–600 °C at a heating rate of 2 °C $min^{-1}$. Reaction products were monitored with a gas chromatograph Shimadzu GC-8A model provided with a TCD detector. The separation of products was performed with an Alltech concentric column CTRI. This system permits the identification and quantification of $O_2$, $N_2$, $CO_2$ and CO peaks.

## 3. Results and discussion

### 3.1. Transformations occurring during the calcination of precursors

Transformations occurring during the calcination of precursors containing lithium nitrate were studied by TGA and DSC. Fig. 1 shows the results of experiments performed with lithium nitrate bulk. Curve (a) of Fig. 1 corresponds to a TGA diagram and curve (b) corresponds to a DSC experiment. The salt starts melting at 247.4 °C and the minimum is centered at 259.5 °C. The decomposition process of lithium nitrate starts at 485 °C.

The decomposition of lithium nitrate can give either lithium oxide or peroxide and the corresponding nitrogen oxides.

When decomposition occurs with the formation of lithium oxide, the mass loss should be 78.3% and when it decomposes giving lithium peroxide the mass loss should be 66.7%.

The maximum mass loss obtained experimentally during calcination of the lithium nitrate bulk (curve a) is 75.5% and occurs at 650 °C. Then the mass increases with temperature and the mass loss from room temperature up to 850 °C is 64.3%. These results point

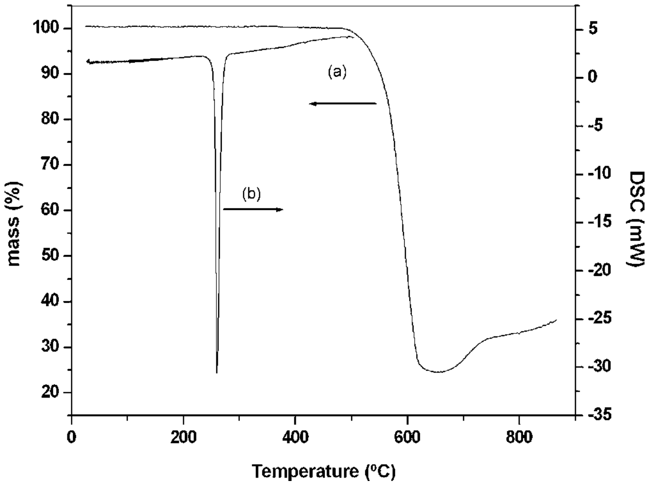

**Fig. 1.** TGA diagrams (curve a, mass: 1.07 mg) and DSC (curve b, mass: 0.7 mg) of $LiNO_3$ salt bulk.

to the formation of lithium oxide up to 650 °C. When this decomposition was carried out by mass spectroscopy, it was possible to observe fragments of $m/z = 30$ which is the signal of higher intensity in mass spectra of $NO_2$ and NO. At higher temperatures this oxide is further oxidized giving the corresponding peroxide. These results would indicate that part of the lithium nitrate is not decomposed in the time interval.

Fig. 2 shows the DSC diagrams of precursors prepared by lithium nitrate impregnation on different supports. The DSC curve of the $LiNO_3$ bulk (Fig. 1) shows that melting starts at 247.4 °C and the signal is observed at 246.9 °C for the $PLiNO_3/ZrO_2$ precursor. The heat required to melt the bulk salt and supported salt on zirconium oxide is 79.8 and 77.0 cal $g^{-1}$, respectively. These similar results indicate that the salt is found on the $ZrO_2$ support without interacting.

The DSC diagrams of the $PLiNO_3/SiO_2$ and $PLiNO_3/ZrO_2{\cdot}nH_2O$ precursors (Fig. 2, curves (a) and (c), respectively) do not show any melting signal in the 247.4 °C range. These results show that lithium nitrate is found to be either highly dispersed on the support or strongly interacting with it, and does not present the classical phenomenon of crystal melting at 247.4 °C.

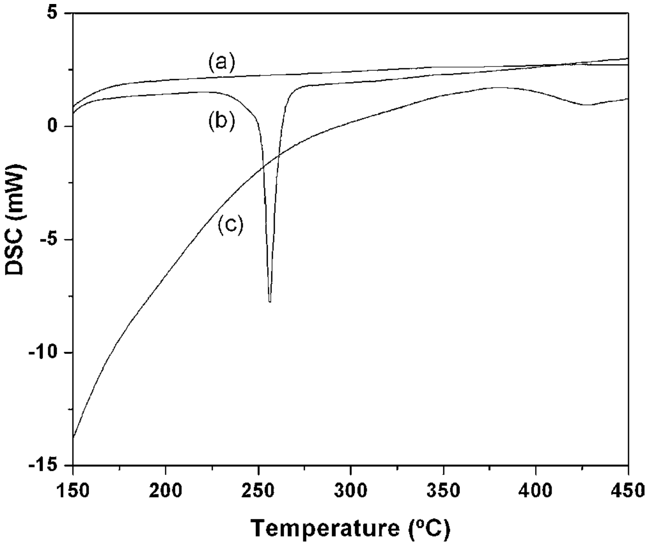

**Fig. 2.** DSC of $LiNO_3$/support precursors. (a) $PLiNO_3/SiO_2$, (b) $PLiNO_3/ZrO_2$ and (c) $PLiNO_3/ZrO_2{\cdot}nH_2O$.

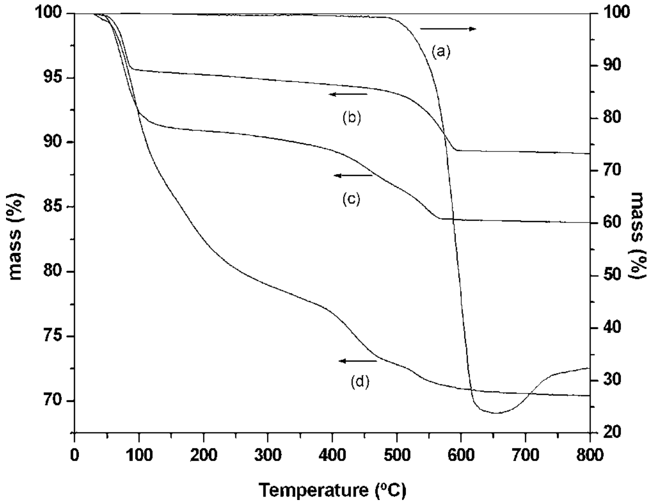

**Fig. 3.** TGA diagrams of $LiNO_3$ (mass: 1.07 mg) and $LiNO_3$/support precursors (mass: 10 mg). (a) $LiNO_3$, (b) $LiNO_3/ZrO_2$, (c) $LiNO_3/SiO_2$ and (d) $LiNO_3/ZrO_2{\cdot}nH_2O$.

The XRD pattern of the $PLiNO_3/ZrO_2$ catalytic precursor shows diffraction lines typical of $LiNO_3$. These diffraction lines cannot be observed in precursors obtained by impregnation of high area supports ($SiO_2$ and $ZrO_2{\cdot}nH_2O$). The absence of signals in XRD indicates that $LiNO_3$ crystals are not detectable by the technique.

In DSC experiments, it is clearly observed a melting signal of $LiNO_3$ in the $PLiNO_3/ZrO_2$ and in the XRD experiment, the crystalline phase is observed. For precursors $PLiNO_3/SiO_2$ $PLiNO_3/ZrO_2{\cdot}nH_2O$ no signals are observed in XRD indicating high salt dispersion and no melting signals in DSC are noticed.

Fig. 3 shows the TGA diagrams of the $LiNO_3$ bulk and precursors. TGA curves of the bulk salt and the supported precursor on $ZrO_2$ are similar. While the lithium nitrate bulk increases in mass from 650 °C, none of the precursors display this property. These results would indicate that part of the supported lithium nitrate decomposes to lithium oxide but it is not transformed into peroxide at higher temperatures. These results coincide with those found by Bothe-Almquist et al. [17]. Although these authors found lithium peroxide in the catalysts prepared from LiCl and LiOH, they did not find lithium peroxide in the catalysts prepared by impregnation with $LiNO_3$.

### 3.2. *Characterization of catalysts*

#### 3.2.1. *Estimation of the remaining lithium nitrate with TGA experiments*

In order to estimate the remaining lithium nitrate content in the catalysts, a TGA was carried out in an air flow heated to 600 °C, which was maintained at this temperature for 30 min.

In each TGA diagram, the mass loss was calculated from 200 °C to the end of the experiment (600 °C for 30 min calcination). It is supposed that lithium nitrate decomposes to give lithium oxide, as indicated by the previous thermogravimetry experiments, which were carried out up to 800 °C. Thus, if the amount of lithium nitrate transformed into lithium oxide is calculated, then the remaining lithium nitrate can be determined by the difference between the amount of lithium oxide formed and the amount of lithium nitrate impregnated in the precursors (8.34%, w/w). Mass losses of supports were taken into account.

Table 1 shows the content of the remaining lithium nitrate estimated by TGA. For the precursor impregnated on $ZrO_2{\cdot}nH_2O$, no estimates were performed because the support contains water molecules that are lost during the TGA experiment. Table 1 also shows the results of measurements of nitrate (Colorimeter DR/890 Hach equipment) and lithium (atomic absorption spectrometry).

**Table 1**
Lithium and lithium nitrate content in catalysts.

| Sample | TGA % $LiNO_3$ remaining | Colorimeter Soluble $\%NO_3$ | AA spectrometry % Li |
|---|---|---|---|
| $LiNO_3/SiO_2$ | 0.52 | 0.78 | 0.74 |
| $LiNO_3/ZrO_2$ | 1.00 | 0.63 | 0.80 |
| $LiNO_3/ZrO_{2(tetra)}$ | – | 0.45 | 0.50 |

Precursors were impregnated with 8.34% lithium nitrate and the concentration of the remaining and soluble lithium nitrate in the catalysts varied between 0.45 and 0.78%.

The lithium concentration in the $LiNO_3/SiO_2$ and $LiNO_3/ZrO_2$ catalysts is similar to the nominal lithium concentration (0.84%), on the other hand, in the catalyst prepared by impregnation on $ZrO_2{\cdot}nH_2O$, the measurement of lithium content showed that it decreased. This would indicate that during precursor calcinations at 600 °C, part of lithium nitrate can be lost by volatilization.

### 3.2.2. *X-ray diffraction*

Fig. 4 shows the XRD patterns of the three catalysts and also the diagram for the zirconia support. Reflection lines corresponding only to the supports are observed in the diffractograms. The diffractogram of the $LiNO_3/ZrO_2$ catalyst displays reflections of crystallized zirconia in a monoclinic phase with the principal peaks at $2\theta = 28.2°$, 31.5° and 34.5°, while the catalyst prepared from $ZrO_2{\cdot}nH_2O$ shows peaks corresponding to metastable tetragonal zirconia with the principal peaks at $2\theta = 30.5°$, 35.2° and 50.7°. Signals of $LiNO_3$ ($2\theta = 24.7°$, 32.0° and 42.3°) and $Li_2O$ ($2\theta = 33.8°$) are not observed because the concentration in the catalysts is too low to be observed by this technique. On the other hand, XRD lines of lithium silicates and zirconates are not observed.

### 3.2.3. *Infrared spectroscopy (FTIR)*

The free $NO_3^-$ anion has a relatively high symmetry ($D_{3h}$) and consequently it has a simple infrared spectrum. It gives a vibration mode of anti-symmetric stretching ($\nu_{as}$) at about 1380 cm$^{-1}$ and this energy absorption path is the one that can be considered as the most intense. The symmetric vibration mode ($\nu_s$) is inactive in IR. There are two modes of angular deformation O–N–O active in IR at 830 and 720 cm$^{-1}$. A shift and an unfolding of the anti-symmetric stretching band are observed toward higher frequencies (1400 and 1500 or 1600 cm$^{-1}$) if nitrate is found as either a mono or bidentate ion [14,15].

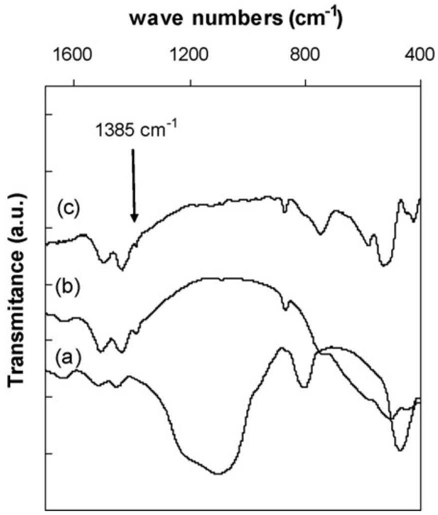

**Fig. 5.** FTIR spectra of catalysts and lithium nitrate. (a) $LiNO_3/SiO_2$, (b) $LiNO_3/ZrO_{2(tetra)}$ and (c) $LiNO_3/ZrO_2$.

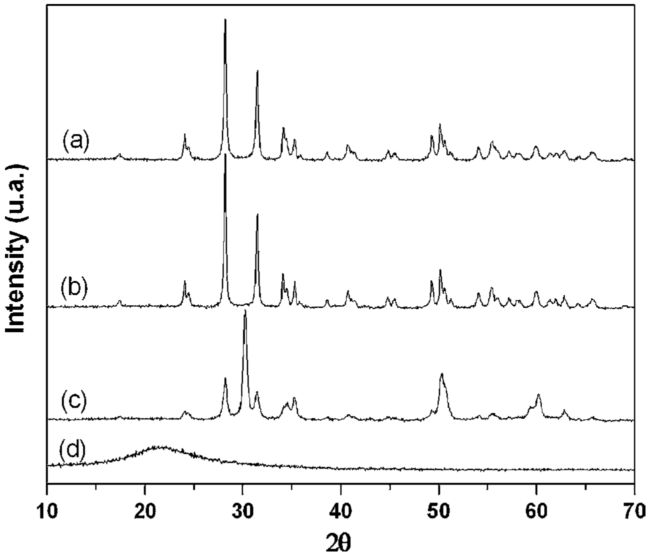

**Fig. 4.** X ray diffraction diagrams. (a) $ZrO_2$, (b) $LiNO_3/ZrO_2$, (c) $LiNO_3/ZrO_{2(tetra)}$ and (d) $LiNO_3/SiO_2$.

Fig. 5 shows the FTIR spectra of the catalysts. The spectra for the $LiNO_3/ZrO_{2(tetra)}$ and $LiNO_3/ZrO_2$ catalysts show a small energy absorption band at 1385 cm$^{-1}$ associated with the $\nu_{as}$ mode, which is typical of free nitrate ions. Also, bands at 1420 and 1490 are observed and attributed to the presence of monodentate nitrate ions coordinated with the support.

The IR spectrum of the $LiNO_3/SiO_2$ catalyst clearly shows the vibrational spectrum of $SiO_4$ tetrahedrons with energy adsorption bands at 790, 957 and 1092 cm$^{-1}$. In this catalyst, the band associated with the presence of free nitrate ions (1385 cm$^{-1}$) cannot be observed and it is possible to see bands at 1436 and 1505 cm$^{-1}$. These signals are assigned to the presence of a $NO_3^-$ species interacting with the support [16].

### 3.2.4. *Photoelectronic spectroscopy (XPS)*

The XPS analysis provides information about lithium compounds present on the catalyst surface as well as the superficial lithium concentration.

Fig. 6 shows the XPS spectra in the BE region between 48 and 63 eV where signals corresponding to lithium species are found. In the spectra of the $LiNO_3/SiO_2$ and $LiNO_3/ZrO_2$ catalysts it is possible to note a peak with a BE of 55.4 eV, but this signal is largely over-

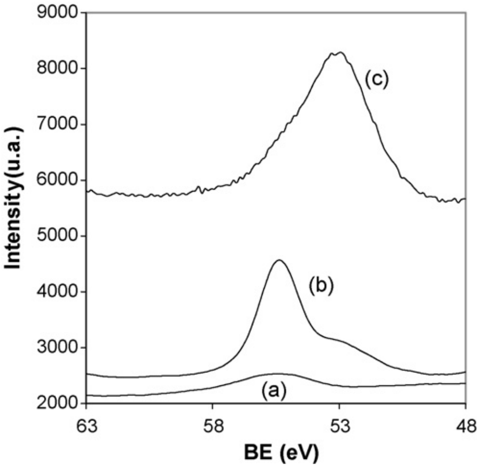

**Fig. 6.** XPS of lithium 1s. (a)$LiNO_3/SiO_2$, (b) $LiNO_3/ZrO_2$ and (c) $LiNO_3/ZrO_{2(tetra)}$.

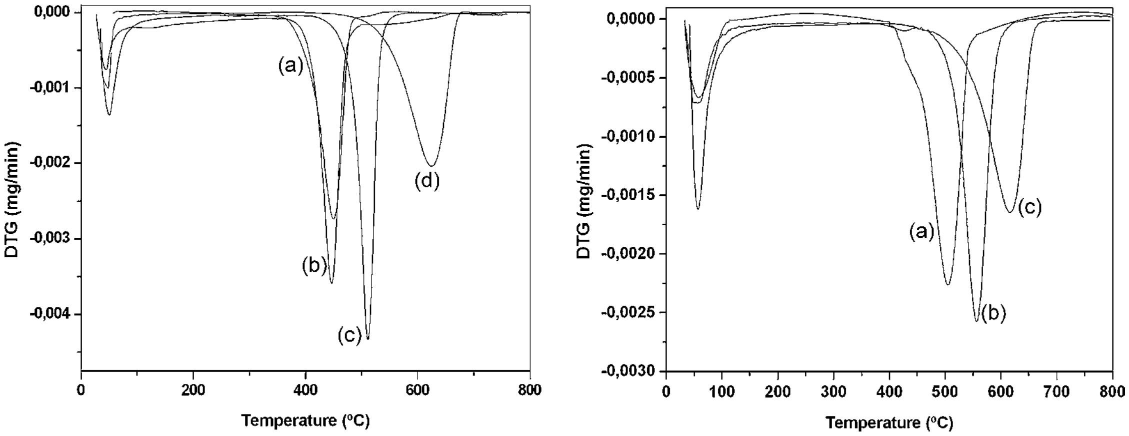

**Fig. 7.** (A) Support influence in soot combustion. (a)$LiNO_3/ZrO_2$, (b) $LiNO_3/ZrO_{2(tetra)}$, (c) $LiNO_3/SiO_2$ and (d) soot. (B) Soot combustion rate. $Li_2O$/support catalysts. (a) $Li_2O/ZrO_2$, (b) $Li_2O/SiO_2$ and (c) $Li_2O/ZrO_{2(tetra)}$.

lapped by the Zr 3p signal in the $LiNO_3/ZrO_{2(tetra)}$ catalyst. This fact makes it difficult the quantification of the superficial content. However, the lithium signal is presented with higher intensity in the spectrum of $LiNO_3/ZrO_2$ catalyst. This result suggests that this catalyst presents higher surface concentration of lithium ion than the other two ones. In the spectra of the $LiNO_3/SiO_2$ this signal presents the lower intensity indicating a low surface concentration.

Nitrate signals were not found by this technique, the results being in agreement with observations of Hirata et al. [17]. Nitrate ions can however be observed if special measurements are made consisting of gathering information using very short exposure times.

### 3.3. *Catalytic activity*

#### 3.3.1. *Activity measurements with air in the feed*

Fig. 7a shows the TG-DTG diagrams of all the catalysts prepared, performed in a thermobalance. A soot combustion curve without any catalyst is also included.

In order to investigate the effect of nitrate ions, the DTG results were compared with the soot combustion using catalysts with the same nominal lithium content but prepared from lithium hydroxide. In Fig. 7b the results of the soot combustion experiments are shown using $Li_2O/SiO_2$, $Li_2O/ZrO_2$ and $Li_2O/ZrO_{2(tetra)}$ catalysts.

The results show the evidently higher activity of the catalysts containing a remainder of lithium nitrate [9,10], and the catalysts prepared from lithium nitrate are more active than those prepared from lithium hydroxide.

The temperature of maximum combustion rate (Tmax) for the $Li_2O/SiO_2$ catalyst is 556 °C, while for the $LiNO_3/SiO_2$ catalyst, the maximum occurs at 510 °C.

$Li_2O/ZrO_2$ catalyst presents the temperature of maximum combustion rate (Tmax) at 505 °C, while for the $LiNO_3/ZrO_2$ catalyst, the maximum occurs at 450 °C.

The difference is more noticeable when the support is tetragonal $ZrO_2$; the Tmax for the combustion with the $Li_2O/ZrO_{2(tetra)}$ catalyst is 617 °C, and the combustion with the $LiNO_3/ZrO_{2(tetra)}$ catalyst is faster with the Tmax found 170 °C below the previous one. This difference is worthy of note, since the catalyst prepared from lithium nitrate is active in the temperature range that would be found in an exhaust pipe. In contrast, the same does not occur with the catalyst prepared from lithium hydroxide.

#### 3.3.2. *Activity measurements with air and NO in the feed*

Experiments are carried out in a flow microreactor simulating conditions near to the ones found in an exhaust pipe, as loose contact, NO presence in ppm and $O_2$ concentration around 8%.

The combustion in the absence of a catalyst gives its maximum rate at about 590 °C in $NO/O_2$ presence and gives 570 °C in $O_2$ presence.

Fig. 8 shows the results obtained during soot combustion in a flow reactor using a feed mixture that contained 8% $O_2$ in NO presence (1500 ppm) using $LiNO_3$/support catalysts. The reaction starts to become appreciable at 300 °C when using the $LiNO_3/ZrO_2$ and $LiNO_3/ZrO_{2(tetra)}$ catalysts, which display their maximum combustion rate at 367 and 355 °C, respectively. The reaction takes place at a higher temperature when it is catalyzed with $LiNO_3/SiO_2$ which has its maximum burning rate at 467 °C.

Fig. 8 also shows results obtained during soot combustion in a flow reactor using a feed mixture that contained 8% $O_2$ in NO absence and it can be noticed that catalysts show lower activity in these experimental conditions. XPS results show that the surface lithium concentration is higher in catalysts supported on zirconia and particularly on monoclinic zirconia. The activity of these two catalysts in NO absence is similar, which shows that the activity does not correlate with the superficial lithium content but it does with the presence of remaining nitrate.

Table 2 shows the Tmax values when nitrogen oxide is used in the feed and it is comparable to the Tmax when nitrogen oxide is absent from the feed.

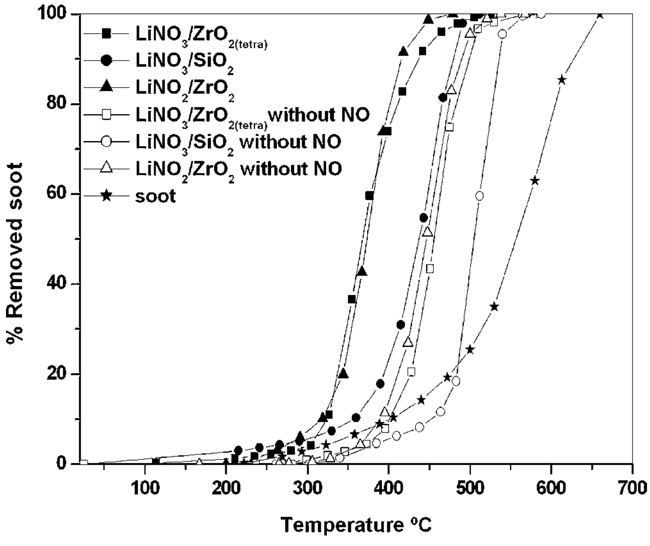

**Fig. 8.** NO influence in soot combustion: (■) $LiNO_3/ZrO_{2(tetra)}$, (▲) $LiNO_3/ZrO_2$ and (●) $LiNO_3/SiO_2$ and in $O_2$ presence: (□) $LiNO_3/ZrO_{2(tetra)}$, (△) $LiNO_3/ZrO_2$ and (○) $LiNO_3/SiO_2$.

**Table 2**
Temperature values for maximum combustion rate (Tmax) obtained in a fixed bed reactor.

| Catalyst | Tmax (°C) in $O_2$ presence | Tmax (°C) in $NO/O_2$ presence | ΔTmax |
|---|---|---|---|
| $LiNO_3/SiO_2$ | 512 | 467 | 45 |
| $LiNO_3/ZrO_2$ | 448 | 367 | 81 |
| $LiNO_3/ZrO_{2(tetra)}$ | 451 | 355 | 96 |

The nitrogen oxide of the feed can react "in situ" with the lithium oxide on the surface giving lithium nitrite which is then oxidized to lithium nitrate. This is the species to which the activity for the soot combustions is attributed, and whose superficial concentration is increased.

$$2NO + Li_2O + 0.5O_2 \rightarrow 2LiNO_2$$

$$2LiNO_2 + O_2 \rightarrow 2LiNO_3$$

The increase in activity resulting from the addition of nitrogen oxide is much more marked in catalysts using zirconia as a support. This result is of great interest since in vehicles using diesel and producing gases containing NO, this product could be eliminated while at the same time promoting catalytic soot combustion.

## 4. Conclusions

The lithium nitrate bulk decomposes in a first stage to lithium oxide and then at temperatures above 650 °C it is further oxidized to lithium peroxide. However, in precursors where lithium nitrate is supported, the transformation of lithium oxide to lithium peroxide is not observed. Catalysts were prepared by calcination of the precursors at 600 °C, and the probable lithium species are lithium oxide and the remaining lithium nitrate which is not decomposed.

By means of thermogravimetry, colorimetry and FTIR techniques, it is possible to demonstrate that part of the lithium nitrate is not decomposed.

Catalysts prepared from lithium nitrate are more active than catalysts prepared from lithium hydroxide and the increase in the reaction rate is attributed to the presence of the remaining lithium nitrate.

Adding NO to the feed accelerates the soot combustion, probably due to the superficial formation of lithium nitrate from nitric oxide, oxygen and lithium oxide.

## Acknowledgements

The authors thank for the financial support of UNSL (Universidad Nacional de San Luis), UNLP (Universidad Nacional de La Plata), CONICET, ANpCYT and Junta de Andalucía Proyecto de Excelencia P06-FQM-01661.

## References

[1] Y. Zhang-Steenwinkel, L.M. van der Zande, H.L. Castricum, A. Blieck, R.W. van den Brink, G.D. Elzinga, Chem. Eng. Sci. 60 (2005) 797.
[2] N. Russo, D. Fino, G. Sarracco, V. Specchia, J. Catal. 229 (2005) 459.
[3] B.A.A.L. van Setten, R. van Dijk, S.J. Jelles, M. Makkee, J.A. Moulijn, Appl. Catal. B 21 (1999) 51.
[4] B.A.A.L. van Setten, C.G.M. Spitters, J. Bremmer, A.M.M. Mulders, M. Makkee, J.A. Moulijn, Appl. Catal. B 42 (2003) 337.
[5] D. Fino, N. Russo, C. Badini, G. Saraco, V. Specchia, AIChE J. 49 (8) (2003) 2173.
[6] N.F. Galdeano, A.L. Carrascull, M.I. Ponzi, I.D. Lick, E.N. Ponzi, Thermochim. Acta 421 (2004) 117.
[7] A.L. Carrascull, M.I. Ponzi, E.N. Ponzi, Ind. Eng. Chem. Res. 42 (2003) 692.
[8] A. Setiabudi, N.K. Allaart, M. Mackkee, J.A. Moulijn, Appl. Catal. B 60 (2005) 241.
[9] A. Carrascull, I.D. Lick, E.N. Ponzi, M.I. Ponzi, Catal. Commun. 4 (2003) 124.
[10] J. Liu, Z. Zhao, C. Xu, A. Duan, L. Zhu, X. Wang, Appl. Catal. B 61 (2005) 39.
[11] N.F. Galdeano, A.L. Carrascull, M.I. Ponzi, I.D. Lick, E.N. Ponzi, Procceding XIX SICAT, México, 2004.
[12] J. van Doorn, J. Varloud, P. Mériaudeau, V. Perrichon, M. Chevrier, C. Gauthier, Appl. Catal. B 1 (1992) 117.
[13] A. Carrascull, C. Grzona, D. Lick, M.I. Ponzi, E.N. Ponzi, React. Kinet. Catal. Lett. 75 (2002) 63.
[14] K.I. Hadjiivanov, Catal Rev. Sci. Eng. 42 (2000) 71.
[15] F.A. Cotton, G. Wilkinson, Química inorgánica avanzada de Ed Limusa Noriega editores, Mexico, 1997.
[16] K. Nakamoto, Infrared and Raman Spectra of Inorganic and Coordination Compounds, Wiley Interscience Publication, John Wiley and sons, Inc., NY, 1997.
[17] M. Hirata, H. Monjyuchiro, R. Sekine, J. Onoe, H. Nakamatsu, T. Mukoyama, H. Adachi, K. Takeuchi, J. Electron Spectros. 83 (1997) 59.